

Lead Oxide Modified Graphite Electrodes for Electrochemical Degradation of Congo Red Dye in Aqueous Solution

Emmanuela Ohanele^{1,2}, Kanayo Oguzie¹, Fabian Ezema^{1,3}, Emeka Oguzie^{1*}

¹ Africa Centre of Excellence in Future Energies and Electrochemical Systems (ACE-FUELS), Federal University of Technology Owerri, PMB 1526, Owerri, Imo State, Nigeria

² Department of Chemical Engineering, Federal Polytechnic Nekede, Owerri 460113, Imo State, Nigeria

³ Department of Physics, University of Nigeria Nsukka, Nsukka 410105, Enugu State, Nigeria

* Corresponding author, e-mail: emaka.oguzie@futo.edu.ng

Received: 21 March 2024, Accepted: 15 July 2024, Published online: 30 August 2024

Abstract

Congo red (CR) dye in aqueous solution was decolorized by an electrolysis process using graphite (G) and lead dioxide modified graphite (G/PbO₂) as anode materials in a two-electrode batch reactor. The electrodeposited lead dioxide film was characterized by scanning electron microscopy coupled with energy dispersive spectroscopy (SEM-EDS) and atomic force microscopy (AFM). Comparative performance assessment of the anode materials under different process parameters reveals that the lead dioxide film improved the electrocatalytic effect of the modified electrode. The adjustment of the deposition bath pH from 1.5 to 3 resulted in the formation of uniform agglomeration and disappearance of particulates, while addition of sodium dodecyl sulphate (SDS) gave better adhesion of film to substrate. The degradation rate (DR) observed for the G/PbO₂ (1.0 × 10⁻² cm²) was higher than that of the unmodified electrode (0.87 × 10⁻² cm²). Increase in applied voltage from 25 to 30 V at 23 mA/mm² improved the degradation efficiency (DE) from 84.7% to 91.32% for graphite and from 96.09% to 99.98% for G/PbO₂, with 0.5 M KCl. The prime degradation time of 45 min was recorded for graphite anode which reduced to 30 min for G/PbO₂ anode. CR degraded to compounds with smaller molecular weight and better stability as observed from GC-MS analysis and computational total energy study, respectively. The modification of the graphite electrode surface by electrodepositing PbO₂ film improved the DE and the prime reaction time. These findings present significant suggestions for the design of advanced electrodeposition and electrocatalytic systems for wastewater treatment applications.

Keywords

electrooxidation, electrodeposition, xenobiotic dye, density functional theory, degradation pathway

1 Introduction

Dyes play a crucial role in various industries, including paint, pulp, cosmetics, and textiles, where they impart color to product. Presently, there are more than 10000 textile dyes in use, with approximately 70% falling into the category of synthetic azo dyes, characterized by their intricate chemical structures [1, 2]. These dyes are classified as electron-deficient xenobiotics due to the presence of electron-withdrawing azo linkages (←N=N→) [3].

The textile industry favors reactive azo dyes for their ability to produce high-quality dyed textiles. However, the aromatic structures inherent in azo dyes confer resistance to natural degradation, leading to their persistence in the environment for extended periods, posing a threat to both flora and fauna [3, 4]. Notably, various illnesses affecting humans and animals have been linked to textile dyes,

known for their high toxicity and potential carcinogenicity [5, 6]. Earlier research, such as Mani's and Bharagava's study in 2016, has explored the toxic, genotoxic, and carcinogenic effects of crystal violet exposure on the environment, along with methods for its degradation and detoxification to ensure environmental safety [7].

Traditional wastewater treatment methods, encompassing physical, chemical, and biological approaches, have limitations, including sludge formation, high time and financial costs [7, 8]. Consequently, there is a pressing need to develop cost-effective and efficient wastewater treatment methods. From the literature, electrochemical oxidation has demonstrated effectiveness in removing organic contaminants from aqueous solutions [9, 10]. Oxidative electrochemical technologies offer promising solutions to

environmental challenges associated with organic pollutants. Among these, anodic oxidation through electrocatalysis, facilitated by *in situ* production of $\bullet\text{OH}$ radicals, has gained prominence due to its advantages, including energy conservation, safety, adaptability, simplicity of use, and environmental compatibility [11, 12]. The rate of electrochemical reactions is significantly influenced by the choice of the electrode material. Therefore, selecting the appropriate electrode material is a critical strategy for enhancing the efficiency of the electrochemical oxidation process. Several materials have been explored as anodes in electrooxidation processes, including metals, like Pt and Ti [13, 14]. Recently, active anodes, like RuO_2 , IrO_2 , and graphite (G) have been used in experimental studies [15]. However, due to their limited capability for oxygen evolution, dimensionally stable anodes (DSA), such as PbO_2 , are considered ideal for wastewater treatment due to their exceptional chemical stability, relatively high overpotential for oxygen evolution, and cost-effectiveness compared to metals or boron-doped diamond (BDD) electrodes [16, 17]. According to Zolfaghari et al., sodium dodecyl sulphate (SDS), an anionic surfactant adsorbs on the surface of nanoparticles to create nanoparticles with negative charges [18]. Li reported that SDS may improve the refinement of the coating particles, boost the oxygen evolution potential (OEP), quicken the charge transfer and significantly enhance the electrocatalytic activity and stability of the PbO_2 electrode [19]. Additionally, Baghal et al. reported that adding SDS to the deposition bath enhanced the absolute surface charge and the adsorption of metals on the substrate. This, in turn, increased the quantity and promoted the uniform distribution of the film deposited [20].

The primary objective of this study is to remediate Congo Red (CR) dye contaminated water using an electrochemical degradation technique which employs lead dioxide modified graphite (G/ PbO_2) electrodes. The PbO_2 electrode was prepared via electrodeposition under varying the pH of the bath. Characterization of the deposited film was performed using SEM-EDS, and AFM analytical techniques. The performance of both the graphite electrode and the modified graphite electrodes was evaluated under different electrolytic conditions. To identify the degradation products, GC-MS was employed, and a computational modeling approach was adapted to predict the thermodynamic energies and stabilities of the intermediate compounds.

2 Methodology

2.1 Chemical and reagents

All chemicals including CR dye, HNO_3 , $\text{Pb}(\text{NO}_3)_2$, HCl, acetone, NaOH, KCl, NaCl, Na_2SO_4 , SDS were used as obtained from JHD Chemical Reagent Co. Ltd. China.

2.2 Pre-treatment of the graphite substrate

Cylindrical graphite rods (10 cm \times 1 cm) used as substrates were mechanically polished using P150C abrasive papers, degreased with acetone in an ultrasonic bath for 10 min, finally rinsed with distilled water and air dried. The rods were then chemically etched in 10 wt% NaOH at 45 °C, 6 V, and 2 A for 20 min to make the surface more adhesive. The graphite rods were ultrasonically cleaned by immersing in 10% HNO_3 for 20 min to remove impurities and then rinsed in distilled water before air drying [21, 22].

2.3 Electrodeposition of lead dioxide nanoparticles on graphite substrate

The electrodeposition solution consists of 0.25 M $\text{Pb}(\text{NO}_3)_2$, 0.25 M HNO_3 , and 0.5 mg/L SDS. The pH of the bath solution was adjusted using 1 M NaOH. The electrical condition of the electrodeposition was the following: constant current of 1.4 A for 60 min in a single-chamber cell with continuous stirring at 60 °C. The pre-treated graphite rod was attached to a 12 V rotor to ensure uniform deposition around the substrate and stainless-steel rods of the same size were used as cathode. After the deposition of PbO_2 , the modified electrode was rinsed multiple times with deionized water and dried in an oven at 60 °C [23].

2.4 Material characterization

The morphology and the chemical composition of the film deposited on the graphite rod was analyzed and characterized using a Phenom Pro Desktop SEM-EDS (ThermoFisher Scientific, USA).

The surface morphology of the modified graphite electrodes, with and without SDS modification, was analyzed before and after use for electrochemical treatment by AFM (Stromlinet Nano Int. Ltd., Denmark) [24, 25].

2.5 Preparation of dye-contaminated water

The CR dye containing wastewater was prepared in the laboratory. The stock solution of 1×10^3 mg/L was further diluted to 30 mg/L with distilled water.

2.6 Electrochemical degradation experiments

A 250 mL single compartment batch reactor was employed for all the electrochemical degradation experiments. The graphite rod (cathode) and the $G/\beta\text{-PbO}_2$ (anode) were of the same dimension and positioned parallel to the sample solution at a distance of 2 cm apart. The setups were continuously agitated at a constant speed of 250 rpm and temperature of 30 °C. NaCl or KCl were used as the supporting electrolyte at different concentrations. After withdrawing 10 mL aliquot of the solution, experiments were conducted galvanostatically with a DC power supply (DAZHENG PS-305D, China). An appropriate aliquot of the reaction solution was taken for analysis at the end of the experiment [26].

2.7 Analytical procedure

A UV-visible spectrophotometer (UV3600 Plus, Perkin Elmer, USA) was used to monitor the residual concentration of CR after electrolysis, using the procedure described elsewhere [27, 28].

A gas chromatograph (Agilent 6890N, USA), and mass spectrometer (Agilent 5973B MSD, USA), was used to identify the chemical constituents present in the CR dye containing water before and after electrolysis and identify the degradation intermediates in the samples [24, 25].

2.8 Computational analysis

The DFT study employed the DMol3 module in Material Studio 2017, with the method specified as LDA/PWC and a COSMO solvation model. The basis set utilized was the Double Numerical plus D-functions basis (DND) 3.5.

3 Results and discussion

3.1 Characterization of PbO_2 electrodeposited film

There are two known polymorphs of PbO_2 obtained via electrodeposition: tetragonal $\beta\text{-PbO}_2$ and orthorhombic $\alpha\text{-PbO}_2$. The crystal structure of PbO_2 deposits is known to be dependent on the pH of the electrodeposition bath. Alkaline bath provides $\alpha\text{-PbO}_2$, while acidic ones provide $\beta\text{-PbO}_2$ [29]. Studies has shown that $\beta\text{-PbO}_2$ exhibited a greater catalytic activity than $\alpha\text{-PbO}_2$ in the degradation of organic pollutants as reported by Chen et al. [29] and Hampson (appears in Ellis et al. [30]).

In this study, a PbO_2 film was deposited on graphite electrode via an electrodeposition procedure, to yield lead dioxide modified graphite (G/PbO_2). Fig. 1 shows the SEM-EDS results for G/PbO_2 films formed when the pH of the electrodeposition bath was varied from pH 1.5 to pH 3 to favor the deposition of $\beta\text{-PbO}_2$ and achieve higher electrocatalytic activity. The EDS spectra show the characteristic signals for

Pb and O on the surface of the graphite electrode at each pH, indicating successful film deposition [29]. This shows that the variations in pH had a substantial impact on the surface morphology of the deposited PbO_2 film.

At pH 2 (Fig. 1(b)), we observed denser, globular-shaped, and flower-like morphology. Higher magnification images revealed well-formed, sparsely deposited particulates with noticeable agglomeration [31]. Additionally, the higher magnification image unveiled the crystalline structure of PbO_2 , showing increased interactions and reduced individual particle boundaries. In Fig. 1(c), there is evidence of agglomeration with reduced individual aggregate boundaries. Remarkably, when the pH of the deposition bath was increased to 3, the PbO_2 particles almost disappeared, resulting in a more uniform morphology [27].

3.2 Effect of anode materials

The study investigated the performance of unmodified and PbO_2 -modified graphite electrodes for electrochemical degradation of CR dye. Fig. 2(a) shows the degradation rate profile for unmodified and PbO_2 -modified graphite electrodes under applied potentials of 25 V and 30 V. The corresponding degradation efficiency profiles are presented in Fig. 2(b), with degradation efficiency values reaching 98% at about 30 min [15, 32]. Degradation efficiency (*DE*) values were obtained from the degradation rate data using equation:

$$DE\% = \frac{C_0 - C}{C_0} \times 100 \quad (1)$$

where C_0 and C are the concentration at time 0 and t , respectively.

The results in Figs. 2(a) and 2(b) show improvement in the degradation performance of graphite electrodes after PbO_2 modification.

The obtained results reveal that G/PbO_2 anode materials outperformed the conventional graphite electrodes in the electrochemical degradation of CR dye. These findings are in accordance with the results published by Moradi et al. [4], who also emphasized the superior performance of PbO_2 based anode materials. The degradation efficiency of 99.98% was achieved after 1 h reaction time, similar to result obtained by Ansari and Nematollahi [33], while Samarghandi et al. reported 96.4% [26].

3.3 Effect of supporting electrolyte

A comparison of the supporting electrolytes was performed with G/PbO_2 at 30 V and 23 mA/mm². As shown in Fig. 3, NaCl achieved 89% *DE* while KCl obtained 98%. These findings indicate that KCl is a more effective

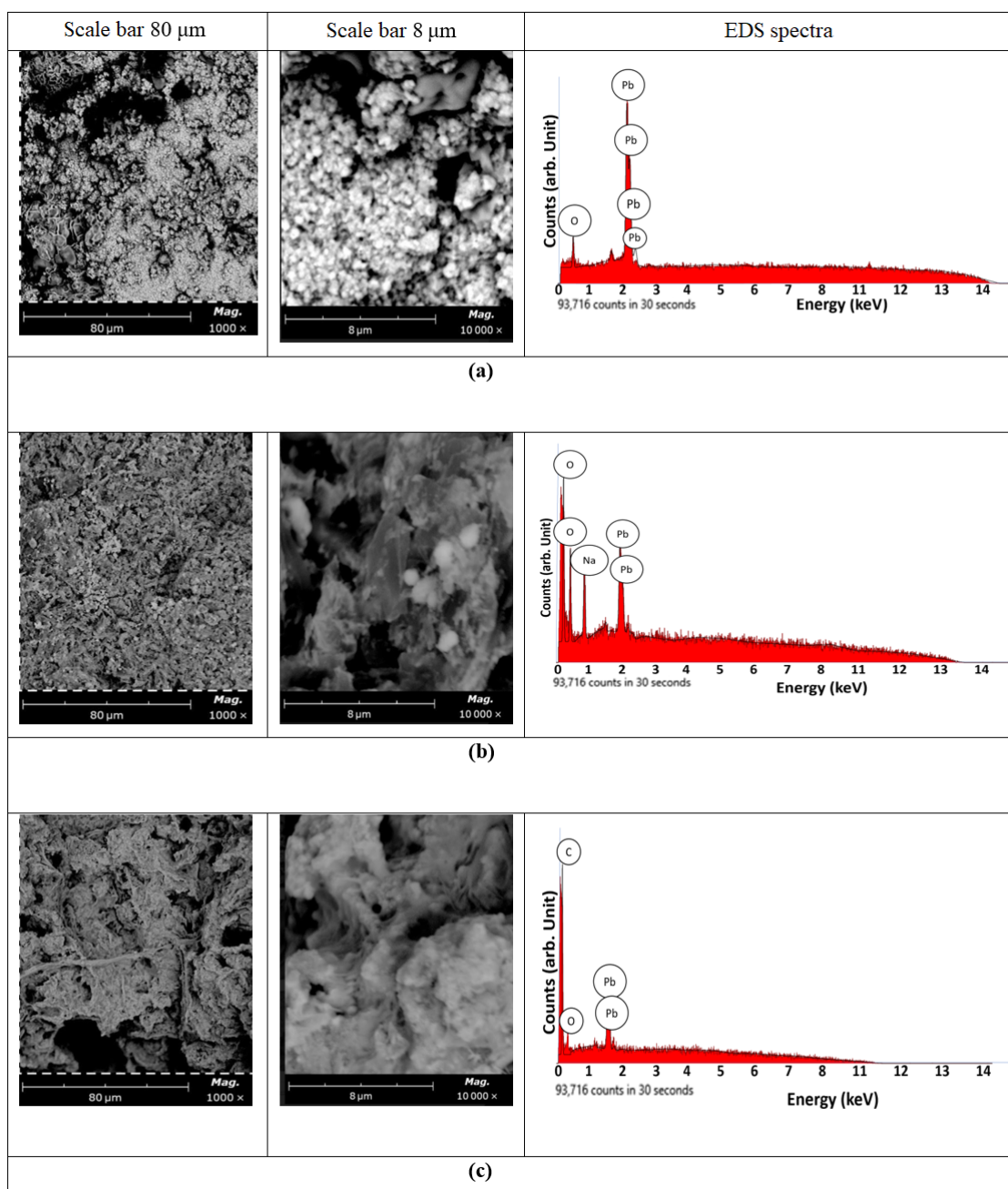


Fig. 1 SEM micrographs and EDS result of G/PbO₂ at pH (a) 1.5 (b) 2 and (c) 3 (bath composition: 0.5g/L SDS, 0.25 M Pb(NO₃)₂, 0.25 M HNO₃)

supportive electrolyte than NaCl. This is consistent with the results reported by Anyanwu et al. [34]. Jalife-Jacobo et al. [35] similarly reported degradation efficiency of 85% after 90 min of CR dye [35].

The superior electrochemical performance of KCl as a supportive electrolyte can be attributed to several factors. Firstly, the difference in the electronegativity between K and Cl is greater than that between Na and Cl. This difference in electronegativity can influence the nature of ion dissociation in solution, which affects the ion mobility and

ionic conductivity. Consequently, KCl offers enhanced ionic conductivity, leading to improved charge transfer at the electrode-electrolyte interface. This, in turn, contributes to more efficient electrochemical reactions and enhanced pollutant degradation [15].

Furthermore, the choice of KCl over NaCl aligns with the well-established principle that cations of higher electropositivity tend to better promote electrochemical processes. The electropositivity of K makes it more favorable for participating in redox reactions compared to Na.

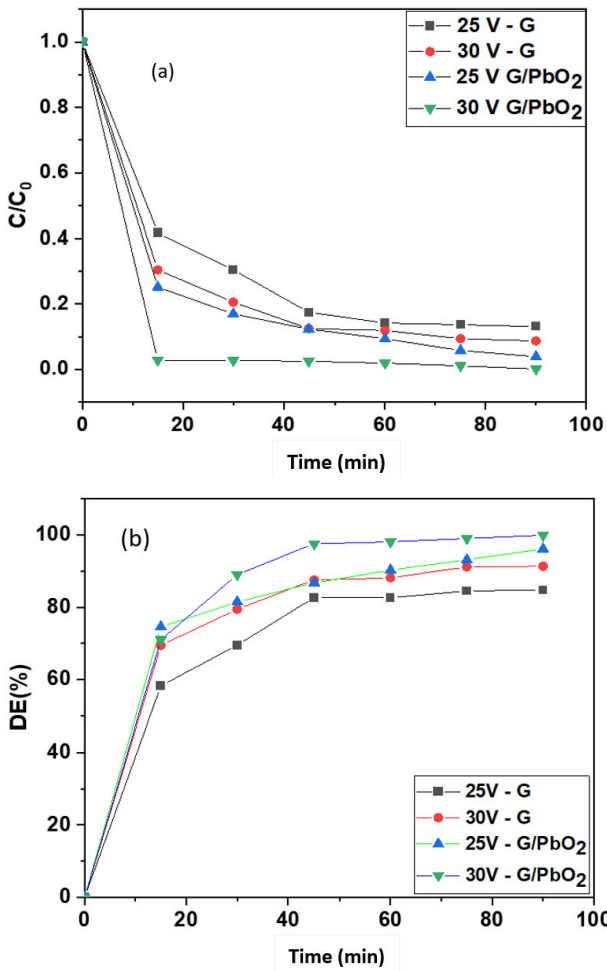


Fig. 2 Effects of PbO₂ modification on (a) the CR dye degradation performance and (b) degradation efficiency of graphite electrode at different potentials (dye conc = 30 mg/L, electrolyte concentration = 1 M KCl, current density = 23 mA/mm², pH = 7, T = 30 °C)

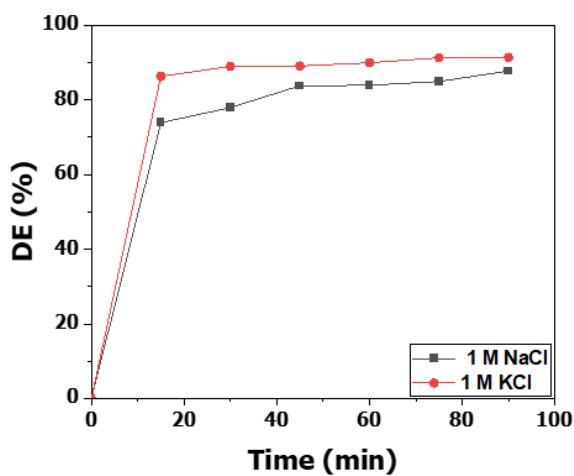


Fig. 3 Effect of supporting electrolyte on CR dye degradation efficiency by PbO₂ modified graphite electrodes (dye concentration = 30 mg/L, current density = 23 mA/mm², pH = 7, T = 30 °C)

3.4 Effect of current density

Current density, a fundamental parameter in electrochemical processes, plays a pivotal role in determining the efficiency and rate of dye degradation. Fig. 4 graphically illustrates the effect of varying current density on *DE* of CR dye using lead dioxide modified graphite (G/PbO₂) anodes in the electrolytic cell. The data presented in Fig. 4 depict an increase in *DE* with increasing applied current density. This phenomenon is in agreement with previous research findings [26]. The improvement in CR dye degradation efficiency with increasing current density can be attributed to several key factors. Previous study [23], has suggested that adjusting current density can affect the formation of oxidizing species, such as the hydroxyl radical ($\bullet\text{OH}$) and hypochlorite (OCl^-), leading to enhanced degradation reactions. The increase in current density is proposed to elevate the production of these oxidizing species while maintaining a constant pH, thus accelerating the reaction. Increasing the current density in our study resulted in shorter electrolysis times and improved efficiency in CR dye degradation. While higher current densities offer advantages in terms of reaction rate and efficiency, it is vital to consider potential limitations like increased energy consumption and electrode wear.

3.5 Kinetic studies

Many kinetic models have been applied to study the controlling mechanism of dye removal from aqueous solution. To correlate the present data with a kinetic first-order rate equation, a graph is plotted between $\ln(C_0/C)$

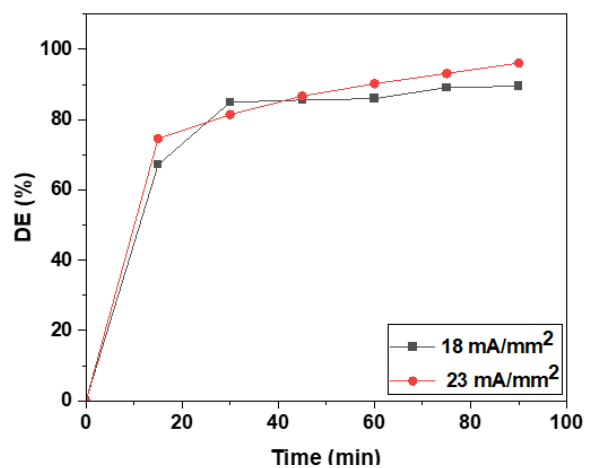


Fig. 4 Effect of current density on Congo red dye degradation efficiency by PbO₂-modified graphite electrodes (dye concentration = 30 mg/L, voltage = 25 V, electrolyte concentration = 1 M KCl, T = 30 °C).

versus time t . The data were then fitted to the first order kinetic equation, given by:

$$\ln \frac{C_0}{C} = K \times t \quad (2)$$

where K is the first order rate constant.

The first-order kinetic plot $\ln(C_0/C)$ vs. t for the electrochemical degradation of CR dye is presented in Fig. 5. The linear plot obtained confirms that the degradation process followed the first order kinetic law, with rate constant is 2.6×10^{-5} 1/s.

Further kinetic evaluation involved the estimation of the normalized space velocity (S_n), which is a crucial parameter that is used to evaluate the efficacy of electrochemical wastewater treatment cells. It is related to the design of the cell and is defined as the volume of wastewater in mL for which the concentration of the waste can be reduced by a factor of 10 in a single second within a reactor capacity of 1 mL. It expresses how fast the reactants are flowing through the reactor relative to the reactor volume and the anode active area.

According to [36] the normalized space velocity is given by:

$$S_n = \frac{I \times \phi}{\Delta C \times V_R \times ZF} \log \frac{C_0}{C} \quad (3)$$

where:

- I : current;
- ϕ : overall current efficiency;
- ΔC : concentration change across the reactor;
- V_R : volume of the reactor;
- ZF : Faraday's constant.

For the electrochemical cell of a batch reactor, Eq. (3) is expressed as [37, 38]:

$$S_n = \frac{K \times A}{2.3 \times V_R} \quad (4)$$

K is 2.6×10^{-5} 1/s, A is the active anode area (22 cm^2), and V_R is 250 mL. The obtained value of the normalized space velocity is: $S_n = 9.95 \times 10^{-7}$ cm/s.

3.6 AFM morphological analysis

The AFM surface morphology of the G/PbO₂ film without and with SDS modification, including the computed values of the average roughness, are shown in Fig. 6.

The AFM images before application Fig. 6(a)–(c) show that the modification gave the electrode a polished finishing which confirms the film deposition. As expected the

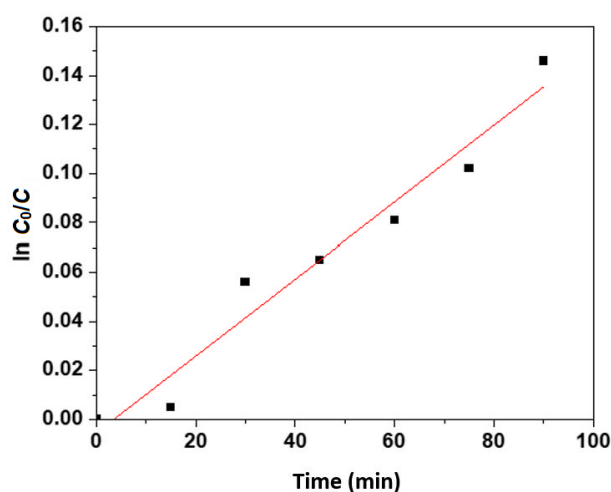


Fig. 5 The plot of $\ln C_0/C$ against time (first order decay)
($K = 2.6 \times 10^{-5}$ 1/s)

average roughness decreased with deposition on the substrate and it is the lowest when SDS was also added [39].

The topography of the electrode surface after application shows spike like protrusions covering the surface [40].

The average roughness of the unmodified electrode decreased significantly after the application of the electrode in CR dye electrooxidation. This indicates that the film was eroded [41]. However, for electrode modified with SDS, the average roughness decreased slightly after the electrode was applied. The roughness decreased due to poor adhesion of the film deposited without SDS. The slight change of roughness observed for SDS modified electrode suggests the better adhesion of the deposited film to the substrate [41].

3.7 Computational analysis

DFT simulations were used to examine the susceptible attack sites on the CR molecular structure and degradation initiation as shown in Fig. 7.

The highest occupied molecular orbital (HOMO) value is directly related to the ability of the molecule to donate electrons, while the lowest unoccupied molecular orbital (LUMO) value is inversely related to its electron-accepting capacity. These relationships emphasize the critical role of HOMO and LUMO values in understanding the electrochemical degradation mechanism of CR.

Additionally, we employed the Fukui indices (FI) to assess the reactive regions of the CR molecule in terms of nucleophilic (F^+), electrophilic (F^-), and radical (F^0) susceptibilities. This analysis helped us to identify the active sites which likely initiate the oxidative process, as detailed in Table S1 of the Supplement, using the Hirshfeld population analysis (Materials studio).

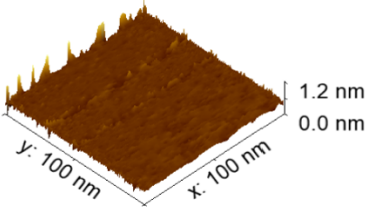
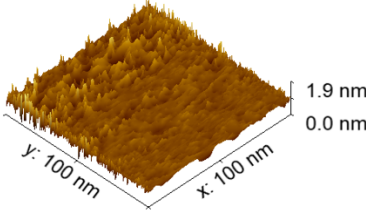
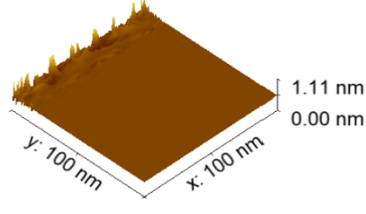
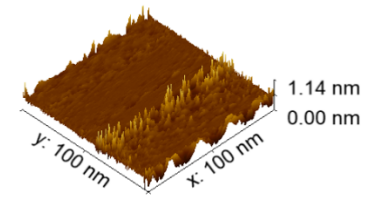
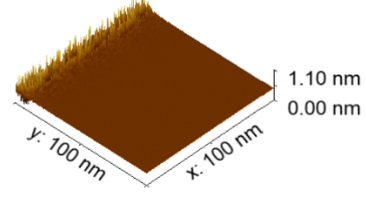
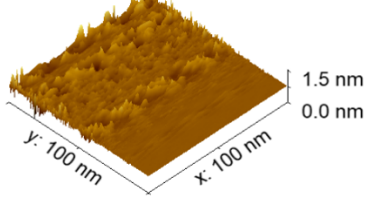
	Before Electrolysis	After Electrolysis
(a) Graphite Electrode as purchased	 <p>Average roughness: 0.89082 μm</p>	 <p>Average roughness: 0.03776 μm</p>
(b) Without SDS modification	 <p>Average roughness: 0.78785 μm</p>	 <p>Average roughness: 0.4440 μm</p>
(c) With SDS Modification	 <p>Average roughness: 0.60039 μm</p>	 <p>Average roughness: 0.46441 μm</p>

Fig. 6 AFM images of the G/PbO₂ modified electrode surface (a) modified without SDS before application, (b) modified without SDS after application, (c) modified with SDS before application and, (d) modified with SDS after application. The images were obtained in tapping mode.

Table S2 reveals that the nitrogen atoms exhibit the highest FI values, indicating their susceptibility to attack. This susceptibility aligns with the presence of the $-\text{N}=\text{N}-$ group in the azo structure. Notably, the attack predominantly targets the naphthylamine and benzidine aromatic amine groups within the CR dye structure, as previously reported by Maruthapandi et al. [42].

3.8 Degradation pathway

GC-MS fragmentation analysis identified various intermediates, confirming the breakdown of the entire dye into smaller, low-molecular-weight compounds. The specific peak compounds are listed in Table S2 in the Supplement. Furthermore, the intermediates generated during the electrochemical treatment of CR dye indicated the absence of azo bonds ($-\text{N}=\text{N}-$) and phenolic compounds after 45 min

of degradation. This observation underscores the successful dissolution of the azo bond within the chemical structure of CR dye [43].

Following the GC-MS analysis and computational results, it can be inferred that the chromophoric groups underwent oxidation to form sulphonamide compounds, which were subsequently broken down into aldehydes. This breakdown led to the opening of the aromatic rings, resulting in the formation of primary alcohols and alkanes. Mineralization processes then occurred, ultimately yielding carbon dioxide and water as the end products. Fig. S1 and Fig S2 are the graphic representation of the electrochemical degradation profile of CR dye by unmodified and the modified electrode at different current densities and different supporting electrolytes. The proposed degradation pathway is illustrated in Fig. S3.

anti-corrosion effect of the coating. The degradation rate observed for the G/PbO₂ was higher than for the unmodified graphite electrode. Increase in the applied voltage from 25 to 30 V at 23 mA/mm² improved the *DE* from 84.7% to 91.32% for graphite and from 96.09% to 99.98% and for G/PbO₂, respectively with 1 M KCl. The most favorable degradation time of 45 min was recorded for graphite anode system but reduced to 30 min with G/PbO₂ anode electrolytic cell. CR degraded to compounds with smaller molecular weights as the different intermediate compounds was

dictated with GC-MS. The theoretical energy study of the degradation products showed that the compounds are more stable than CR dye.

Acknowledgement

The authors gratefully acknowledge financial support from the World Bank and French Development Agency, within the framework of the Second Africa Higher Education Centers of Excellence for Development Impact (ACE Impact) Project – P169064, IDA No 6510-NG.

References

- [1] Hassan, M. M., Carr, C. M. "A critical review on recent advancements of the removal of reactive dyes from dyehouse effluent by ion-exchange adsorbents", *Chemosphere*, 209, pp. 201–219, 2018. <https://doi.org/10.1016/j.chemosphere.2018.06.043>
- [2] Gul, S., Afsar, S., Gul, H., Ali, B. "Removal of crystal violet dye from wastewater using low-cost biosorbent *Trifolium repens* stem powder", *Journal of the Iranian Chemical Society*, 20(11), pp. 2781–2792, 2023. <https://doi.org/10.1007/s13738-023-02875-x>
- [3] Singh, J., Kalamdhad, A. S., Koduru, J. R. "Potential degradation of hazardous dye Congo red by nano-metallic particles synthesized from the automobile shredder residue", *Nanotechnology for Environmental Engineering*, 2(1), 10, 2017. <https://doi.org/10.1007/s41204-017-0021-z>
- [4] Moradi, M., Vasseghian, Y., Khataee, A., Kobya, M., Arabzade, H., Dragoi, E. N. "Service life and stability of electrodes applied in electrochemical advanced oxidation processes: A comprehensive review", *Journal of Industrial and Engineering Chemistry*, 87, pp. 18–39, 2020. <https://doi.org/10.1016/j.jiec.2020.03.038>
- [5] Tounsadi, H., Metarfi, Y., Taleb, M., El Rhazi, K., Rais, Z. "Impact of chemical substances used in textile industry on the employee's health: Epidemiological study", *Ecotoxicology and Environmental Safety*, 197, 110594, 2020. <https://doi.org/10.1016/j.ecoenv.2020.110594>
- [6] Wang, A.-J., Wang, H.-C., Cheng, H.-Y., Liang, B., Liu, W., Han, J., Zhang, B., Wang, S. "Environmental Science and Ecotechnology Electrochemistry-stimulated environmental bioremediation: Development of applicable modular electrode and system scale-up", *Environmental Science and Ecotechnology*, 3, 100050, 2020. <https://doi.org/10.1016/j.ese.2020.100050>
- [7] Mani, S., Bharagava, R. N. "Exposure to Crystal Violet, Its Toxic, Genotoxic and Carcinogenic Effects on Environment and Its Degradation and Detoxification for Environmental Safety", In: de Voogt, W. P. (ed.) *Reviews of Environmental Contamination and Toxicology Volume 237*, Springer Cham, 2016, pp. 71–104. ISBN 978-3-319-23572-1 https://doi.org/10.1007/978-3-319-23573-8_4
- [8] Rashid, R., Shafiq, I., Akhter, P., Iqbal, M. J., Hussain, M. "A state-of-the-art review on wastewater treatment techniques: the effectiveness of adsorption method", *Environmental Science and Pollution Research*, 28(8), pp. 9050–9066, 2021. <https://doi.org/10.1007/s11356-021-12395-x>
- [9] Shindhal, T., Rakholiya, P., Varjani, S., Pandey, A., Hao Ngo, H., Guo, W., Yong Ng, H., Taherzadeh, M. J. "A critical review on advances in the practices and perspectives for the treatment of dye industry wastewater", *Bioengineered*, 12(1), pp. 70–87, 2021. <https://doi.org/10.1080/21655979.2020.1863034>
- [10] Jiang, Y., Zhao, H., Liang, J., Yue, L., Li, T., Luo, Y., Liu, Q., Lu, S., Asiri, A. M., Gong, Z., Sun, X. "Anodic oxidation for the degradation of organic pollutants: Anode materials, operating conditions and mechanisms. A mini review", *Electrochemistry Communication*, 123, 106912, 2021. <https://doi.org/10.1016/j.elecom.2020.106912>
- [11] Jasper, J. T., Yang, Y., Hoffmann, M. R. "Toxic Byproduct Formation during Electrochemical Treatment of Latrine Wastewater", *Environmental Science & Technology*, 51(12), pp. 7111–7119, 2017. <https://doi.org/10.1021/acs.est.7b01002>
- [12] Oturan, M. A., Aaron, J. J. "Advanced oxidation processes in water/wastewater treatment: Principles and applications. A review", *Critical Reviews in Environmental Science & Technology*, 44(23), pp. 2577–2641, 2014. <https://doi.org/10.1080/10643389.2013.829765>
- [13] Fang, C., Megharaj, M., Naidu, R. "Electrochemical Advanced Oxidation Processes (EAOP) to degrade per- and polyfluoro-alkyl substances (PFASs)", *Journal of Advanced Oxidation Technologies*, 20(2), 20170014, 2017. <https://doi.org/10.1515/jaots-2017-0014>
- [14] Feng, Y., Yang, L., Liu, J., Logan, B. E. "Electrochemical technologies for wastewater treatment and resource reclamation", *Environmental Science: Water Research & Technology*, 2(5), pp. 800–831, 2016. <https://doi.org/10.1039/c5ew00289c>

- [15] Kaur, R., Kaur, H. "Electrochemical degradation of Congo red from aqueous solution: Role of graphite anode as electrode material", *Portugaliae Electrochimica Acta*, 34(3), pp. 185–196, 2016. <https://doi.org/10.4152/pea.201603185>
- [16] Cordeiro, J. M. M., de Azevedo, D. H. M., Barretto, T. C. M., Sambrano, J. R. "Conducting behavior of crystalline α -PbO₂ as revealed by DFT calculations", *Materials Research*, 21(1), pp. 1–7, 2018. <https://doi.org/10.1590/1980-5373-MR-2017-0641>
- [17] Zhou, Q., Zhou, X., Zheng, R., Liu, Z., Wang, J. "Application of lead oxide electrodes in wastewater treatment: A review", *Science of the Total Environment*, 806, 150088, 2022. <https://doi.org/10.1016/j.scitotenv.2021.150088>
- [18] Zolfaghari, M., Arab, A., Asghari, A. "Surfactant-Assisted Electrodeposition of Nickel Nanostructures and Their Electrocatalytic Activities Toward Oxidation of Sodium Borohydride, Ethanol, and Methanol", *ChemistrySelect*, 4(15), pp. 4487–4495, 2019. <https://doi.org/10.1002/slct.201900345>
- [19] Li, X., Xu, H., Yan, W. "Effects of twelve sodium dodecyl sulfate (SDS) on electro-catalytic performance and stability of PbO₂ electrode", *Journal of Alloys Compounds*, 718, pp. 386–395, 2017. <https://doi.org/10.1016/j.jallcom.2017.05.147>
- [20] Lari Baghal, S. M., Amadeh, A., Heydarzadeh Sohi, M., Hadavi, S. M. M. "The effect of SDS surfactant on tensile properties of electrodeposited Ni-Co/SiC nanocomposites", *Materials Science and Engineering: A*, 559, pp. 583–590, 2013. <https://doi.org/10.1016/j.msea.2012.08.145>
- [21] Boukhchina, S., Akrouf, H., Berling, D., Boussemli, L. "Highly efficient modified lead oxide electrode using a spin coating/electrodeposition mode on titanium for electrochemical treatment of pharmaceutical pollutant", *Chemosphere*, 221, pp. 356–365, 2019. <https://doi.org/10.1016/j.chemosphere.2019.01.057>
- [22] Zaidi, S. Z. J., Harito, C., Walsh, F. C., Ponce de León, C. "Decolourisation of reactive black-5 at an RVC substrate decorated with PbO₂/TiO₂ nanosheets prepared by anodic electrodeposition", *Journal of Solid State Electrochemistry*, 22(9), pp. 2889–2900, 2018. <https://doi.org/10.1007/s10008-018-3992-1>
- [23] Chen, D., Xiong, F., Zhang, H., Ma, C., Cao, L., Yang, J. "Dimensional Stable Lead Electrode Modified by SDS for Efficient Degradation of Bisphenol A", *ACS Omega*, 5(2), pp. 1198–1205, 2020. <https://doi.org/10.1021/acsomega.9b03571>
- [24] Bian, X., Xia, Y., Zhan, T., Wang, L., Zhou, W., Dai, Q., Chen, J. "Electrochemical removal of amoxicillin using a Cu doped PbO₂ electrode: Electrode characterization, operational parameters optimization and degradation mechanism", *Chemosphere*, 233, pp. 762–770, 2019. <https://doi.org/10.1016/j.chemosphere.2019.05.226>
- [25] Wu, J., Zhu, K., Xu, H., Yan, W. "Electrochemical oxidation of rhodamine B by PbO₂/Sb-SnO₂/TiO₂ nanotube arrays electrode", *Chinese Journal of Catalysis*, 40(6), pp. 917–927, 2019. [https://doi.org/10.1016/S1872-2067\(19\)63342-5](https://doi.org/10.1016/S1872-2067(19)63342-5)
- [26] Samarghandi, M. R., Dargahi, A., Shabanloo, A., Nasab, H. Z., Vaziri, Y., Ansari, A. "Electrochemical degradation of methylene blue dye using a graphite doped PbO₂ anode: Optimization of operational parameters, degradation pathway and improving the biodegradability of textile wastewater", *Arabian Journal of Chemistry*, 13(8), pp. 6847–6864, 2020. <https://doi.org/10.1016/j.arabjc.2020.06.038>
- [27] Panizza, M., Cerisola, G. "Direct and Mediated Anodic oxidation of organic pollutants", *Chemical Reviews*, 109(12), pp. 6541–6569, 2009. <https://doi.org/10.1021/cr9001319>
- [28] Chen, S., Chu, X., Wu, L., Foord, J. S., Hu, J., Hou, H., Yang, J. "Three-Dimensional PbO₂-Modified Carbon Felt Electrode for Efficient Electrocatalytic Oxidation of Phenol Characterized with in Situ ATR-FTIR", *Journal of Physical Chemistry C*, 126(2), pp. 912–921, 2022. <https://doi.org/10.1021/acs.jpcc.1c07444>
- [29] Chen, B. M., Guo, Z. C., Yang, X. W., Cao, Y. D. "Morphology of alpha-lead dioxide electrodeposited on aluminum substrate electrode", *Transactions of Nonferrous Metals Society of China*, 20(1), pp. 97–103, 2010. [https://doi.org/10.1016/S1003-6326\(09\)60103-5](https://doi.org/10.1016/S1003-6326(09)60103-5)
- [30] Ellis, S. R., Hampson, N. A., Ball, M. C., Wilkinson, F. "The lead dioxide electrode", *Journal of Applied Electrochemistry*, 16(2), pp. 159–167, 1986. <https://doi.org/10.1007/BF01093347>
- [31] Khalilzadeh, B., Hasanzadeh, M., Sanati, S., Saghatforoush, L., Shadjou, N., Dolatabadi, J. E. N., Sheikhzadeh, P. "Preparation of a new electrochemical sensor based on cadmium oxide nanoparticles and application for determination of penicillamine", *International Journal of Electrochemical Science*, 6(9), pp. 4164–4175, 2011. [https://doi.org/10.1016/s1452-3981\(23\)18318-0](https://doi.org/10.1016/s1452-3981(23)18318-0)
- [32] Xu, L., Tang, S., Wang, K., Ma, X., Niu, J. "Chemosphere Insights into the degradation and detoxication mechanisms of aqueous capecitabine in electrochemical oxidation process", *Chemosphere*, 241, 125058, 2020. <https://doi.org/10.1016/j.chemosphere.2019.125058>
- [33] Ansari, A. Nematollahi, D. "A comprehensive study on the electrocatalytic degradation, electrochemical behavior and degradation mechanism of malachite green using electrodeposited nanostructured B-PbO₂ electrodes", *Water Research*, 144, pp. 462–473, 2018. <https://doi.org/10.1016/j.watres.2018.07.056>
- [34] Anyanwu, J., Oguzie, K., Oguzie, E., Ogbulie, T. "Electrochemical and microbial treatment of bromophenol blue dye in aqueous solution", *Journal of Electrochemical Science and Engineering*, 13(6), pp. 1063–1080, 2023. <https://doi.org/10.5599/jese.1882>
- [35] Jalife-Jacobo, H., Feria-Reyes, R., Serrano-Torres, O., Gutiérrez-Granados, S., Peralta-Hernández, J. M. "Diazo dye Congo Red degradation using a Boron-doped diamond anode: An experimental study on the effect of supporting electrolytes", *Journal of Hazardous Materials*, 319, pp. 78–83, 2016. <https://doi.org/10.1016/J.JHAZMAT.2016.02.056>

- [36] Perry, S. C., Ponce de León, C., Walsh, F. C. "Review—The Design, Performance and Continuing Development of Electrochemical Reactors for Clean Electrosynthesis", *Journal of The Electrochemical Society*, 167(15), 155525, 2020.
<https://doi.org/10.1149/1945-7111/abc58e>
- [37] Abdel-Aziz, M. H., Bassyouni, M., Zoromba, M. S., Alshehri, A. A. "Removal of Dyes from Waste Solutions by Anodic Oxidation on an Array of Horizontal Graphite Rods Anodes", *Industrial & Engineering Chemistry Research*, 58(2), pp. 1004–1018, 2019.
<https://doi.org/10.1021/acs.iecr.8b05291>
- [38] Walsh, F. C. "Determination of the normalised space velocity for continuous stirred tank electrochemical reactors", *Electrochimica Acta*, 38(2–3), pp. 465–468, 1993.
[https://doi.org/10.1016/0013-4686\(93\)85167-W](https://doi.org/10.1016/0013-4686(93)85167-W)
- [39] Pantić, M., Mitrović, S., Babić, M., Jevremović, D., Kanjevac, T., Džunić, D., Adamović, D. "AFM surface roughness and topography analysis of lithium disilicate glass ceramic", *Tribology in Industry*, 37(4), pp. 391–399, 2015.
- [40] Deng, X., Galli, F., Koper, M. T. M. "In Situ Electrochemical AFM Imaging of a Pt Electrode in Sulfuric Acid under Potential Cycling Conditions", *Journal of American Chemical Society*, 140(41), pp. 13285–13291, 2018.
<https://doi.org/10.1021/jacs.8b07452>
- [41] Ikeuba, A. I. "AFM and EIS investigation of the influence of pH on the corrosion film stability of $\text{Al}_4\text{Cu}_2\text{Mg}_8\text{Si}_7$ intermetallic particle in aqueous solutions", *Applied Surface Science Advances*, 11, 100291, 2022.
<https://doi.org/10.1016/j.apsadv.2022.100291>
- [42] Maruthapandi, M., Saravanan, A., Manohar, P., Luong, J. H. T., Gedanken, A. "Photocatalytic degradation of organic dyes and antimicrobial activities by polyaniline–nitrogen-doped carbon dot nanocomposite", *Nanomaterials*, 11(5), 1128, 2021.
<https://doi.org/10.3390/nano11051128>
- [43] Rafique, M. A., Kiran, S., Javed, S., Ahmad, I., Yousaf, S., Iqbal, N., Afzal, G., Rani, F. "Green synthesis of nickel oxide nanoparticles using *Allium cepa* peels for degradation of Congo red direct dye: An environmental remedial approach", *Water Science and Technology*, 84(10–11), pp. 2793–2804, 2021.
<https://doi.org/10.2166/wst.2021.237>
- [44] Azambou, C. I., Djioko, F. H. K., Obiukwu, O. O., Tsobnang, P. K., Kalu, E. E., Kenfack, I. T., Oguzie, E. E. "Structural, electronic, mechanical and thermodynamic properties of lithium-rich layered oxides cathode materials for lithium-ion battery: Computational study", *Materials Today Communications*, 35, 105738, 2023.
<https://doi.org/10.1016/j.mtcomm.2023.105738>